The Role of Sunspot Rotation in Driving Sigmoid Eruptions

David Alexander and Richard Nightingale

Lockheed Martin Solar and Astrophysics Lab.

Recent observations of rotating sunspots in TRACE white light images and their apparent association with soft X-ray sigmoids have led to the intriguing possibility that the sunspot rotation serves as the driver for both sigmoid formation and their potential eruption. In this paper, we discuss the energization of the corona resulting from currents generated by the vortex motions of the rotating sunspot. We will present a number of events for which we have good white light coverage of the sunspot, an evolving sigmoid and an associated CME (in those cases where the sigmoid erupts). The currents generated by vortex motions in active regions are capable of storing sufficient magnetic energy to power the largest flares and CMEs. We will investigate the relationship between the sunspot rotation and the evolution of the sigmoid structure and attempt to determine the key physical conditions which result in a sigmoid destabilizing and ultimately producing a CME.

Introduction

- In an on-going study, several sunspots, rotating about their umbral centers, have been identified in the TRACE photospheric white light (WL) images (at a 1 arcsec resolution).

  In many cases the rotation can be seen in the corresponding TRACE UV (1600 A) and/or EUV (171, 195A) images, as well as in the MDI data (for 1 case).

  The observations have been derotated and clipped so that all images are co-aligned, and despiking has been performed on the data to remove cosmic ray and particle hits.

  The white light data (for 8-10 August 2000) about the rotating sunspot were 'uncurled' using the geometry shown and displayed as

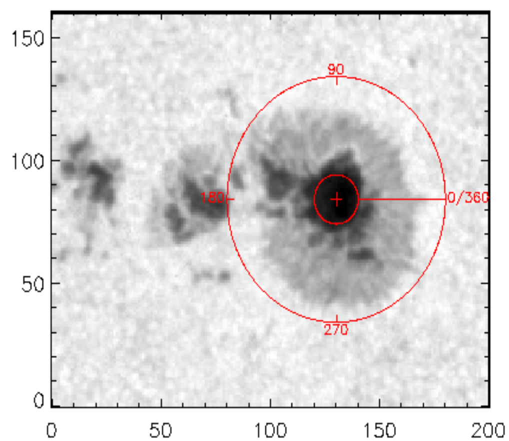

Figure 3: The rotating sunspot can be 'uncurled' by converting from an xy-plot to an $r\theta$-plot. The annulus shown is that used for the plots in figure 4. The angle increases in an anti-clockwise direction.

Introduction II:

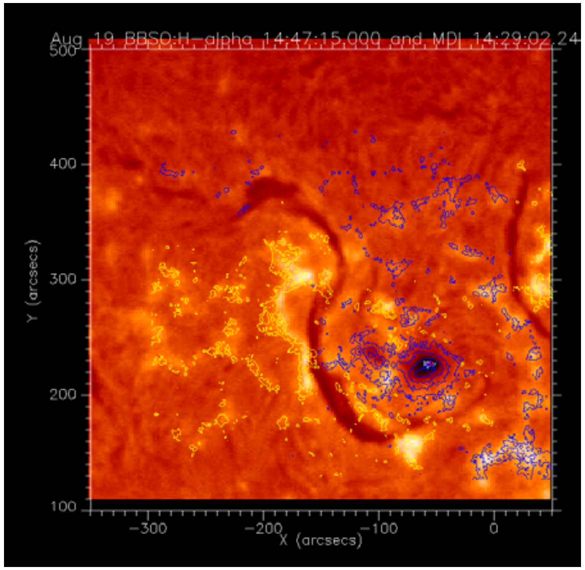

- **In this study we investigate the role of the energization of the corona by sunspot rotation.**
- **The question we want to ask is what, if any, part does the sunspot rotation play in driving a sigmoid to erupt.**
- **In particular, we will investigate `helicity charging' (e.g. Rust and Kumar, 1994a) as a means of energizing and destabilizing the sigmoid.**
- **We consider two distinct observational periods each associated with a well-defined rotation and a sigmoid: 1. Aug 8-10 2000 – sigmoid displayed a wide rangel of activity but no obvious eruption, and 2. Aug15-18 1999 – dynamic sigmoid development with eruption at ~1700 UT on Aug17 (Gibson et al., 2002).**

August 8-10, 2000
(1600 A, 171 A, WL, SOHO/MDI)

Some apparently rotating EUV loops at 171 A caught our attention originally. Then we saw the rotation at several wavelengths.

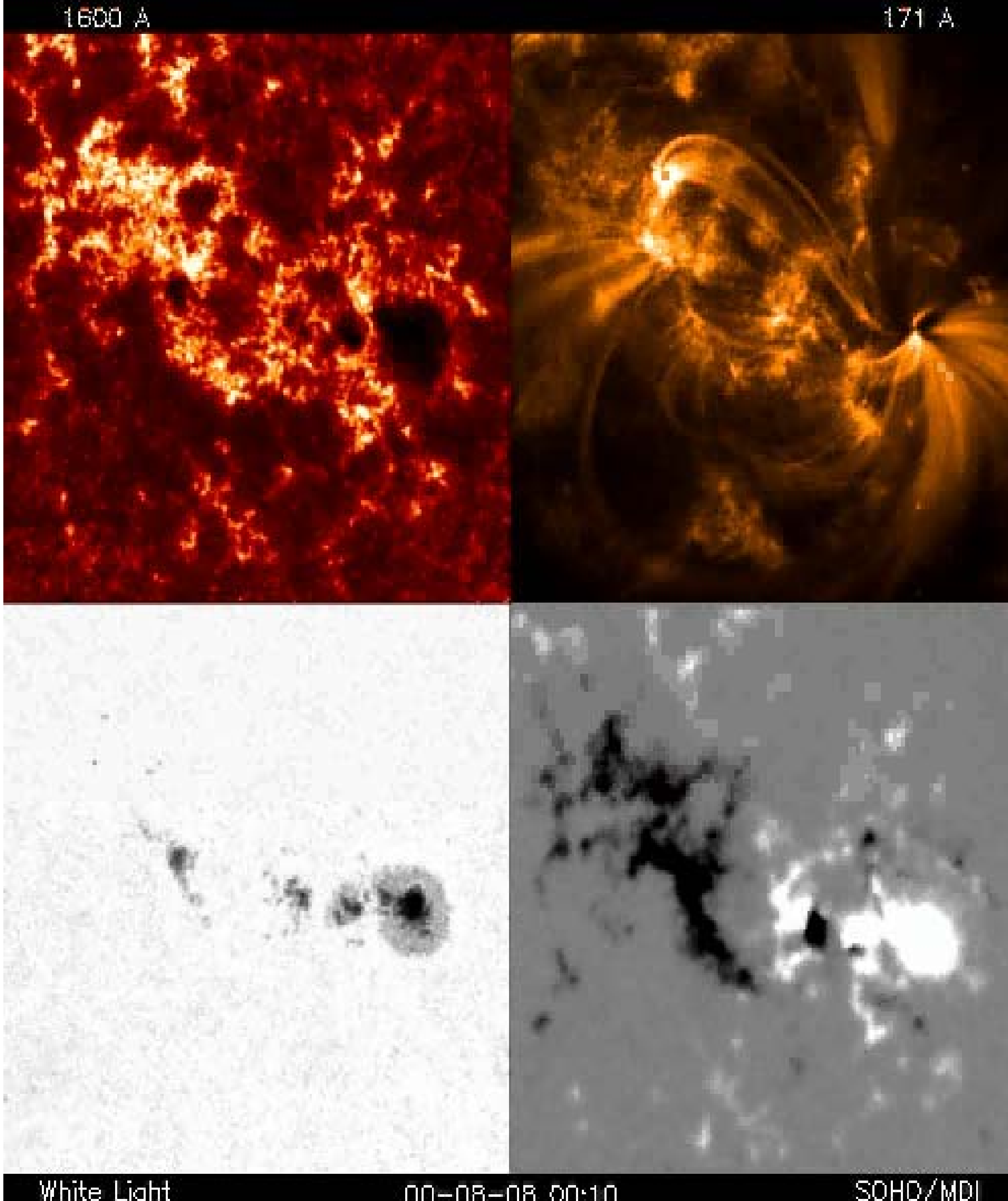

Time slices at different radii were utilized to better display the rotation of other features in and near the sunspot, as appears in this figure at a radius of 15 arcsec for the August 2000 data.

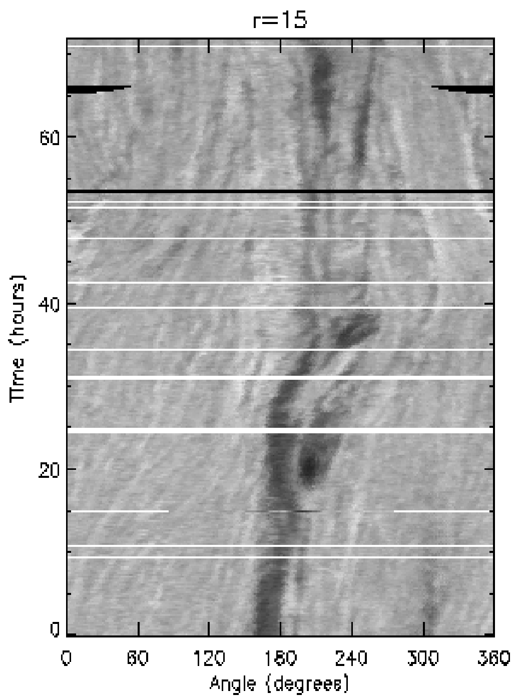

By tracking these features, the rotational speeds at the different times and positions have been calculated. The rotational speed versus radius is shown below for the August 8-10, 2000 event

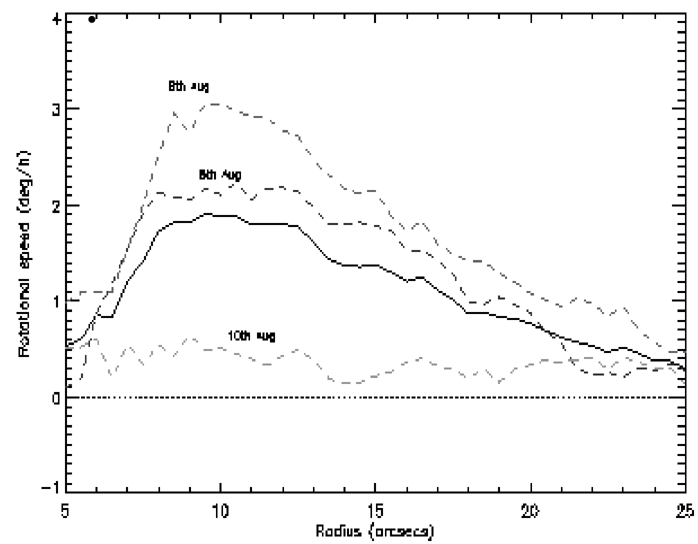

Figure 7: The 3-day average rotational speed in the radial direction is shown by the bold line, while the daily average rotational speeds are given by the dashed lines. The highest rotational rate is between 7-15 arcsecs, which includes the majority of the penumbra of the rotating spot.

The rotational speed versus time and angular spacing are displayed in figures 8 and 9 for August 8-10, 2000.

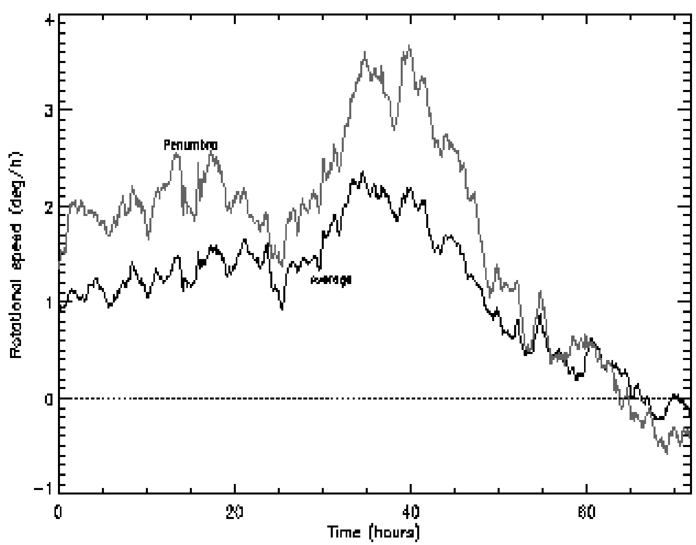

Figure 8: The average rotational speed of the sunspot during the three days observed. The line dubbed 'penumbra' indicates the average speed of the spot in the quicker rotating band between 7-15 arcsecs radius. The bulk of the rotation is on 9th August and there is a sudden drop in speed between 40 and 50 hours, which coincides with the dimming of the sigmoid structure seen in the TRACE 171 Å and Yohkoh data.

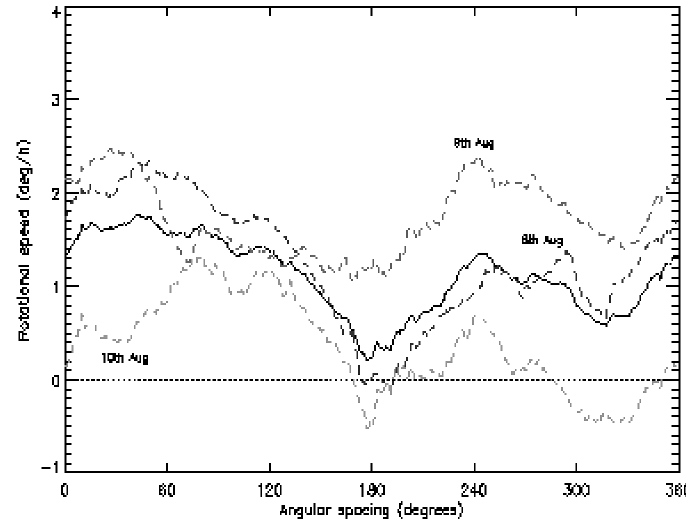

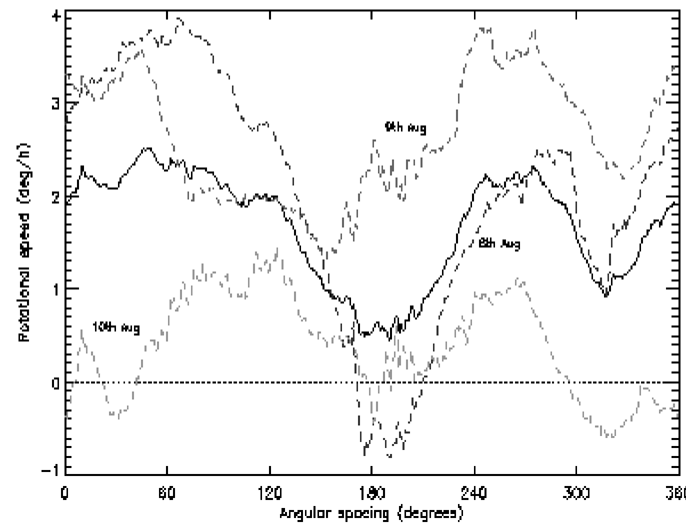

Figure 9: The average rotation of the spot in the angular direction. The lower plot shows the average rotation in the angular direction within the quicker rotational band between 7-15 arcsecs radius. The slowest rotation occurs at 180 degrees, which is where one of the smaller spots lies, this spot undergoes very little rotation compared to the other spot (and smaller penumbral features of the main spot).

Yohkoh SXT on August 8-10, 2000

A selection of corresponding Yohkoh/SXT observations showing that the active region is initially unstressed, but as the rotation occurs a sigmoid forms and then dims, probably due to a

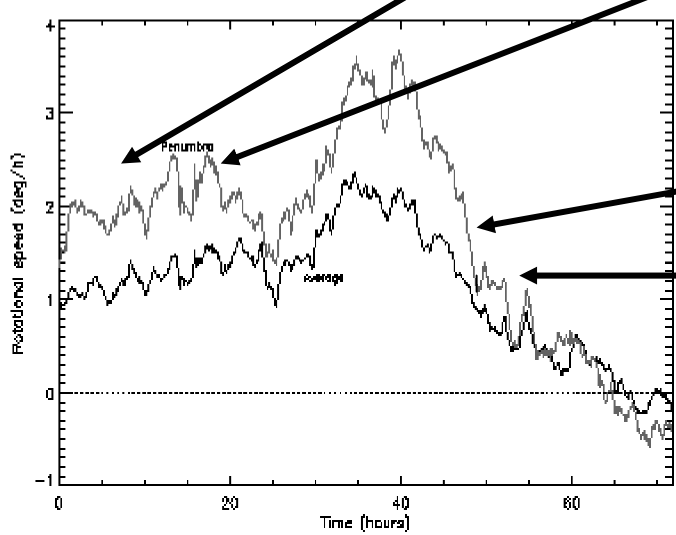

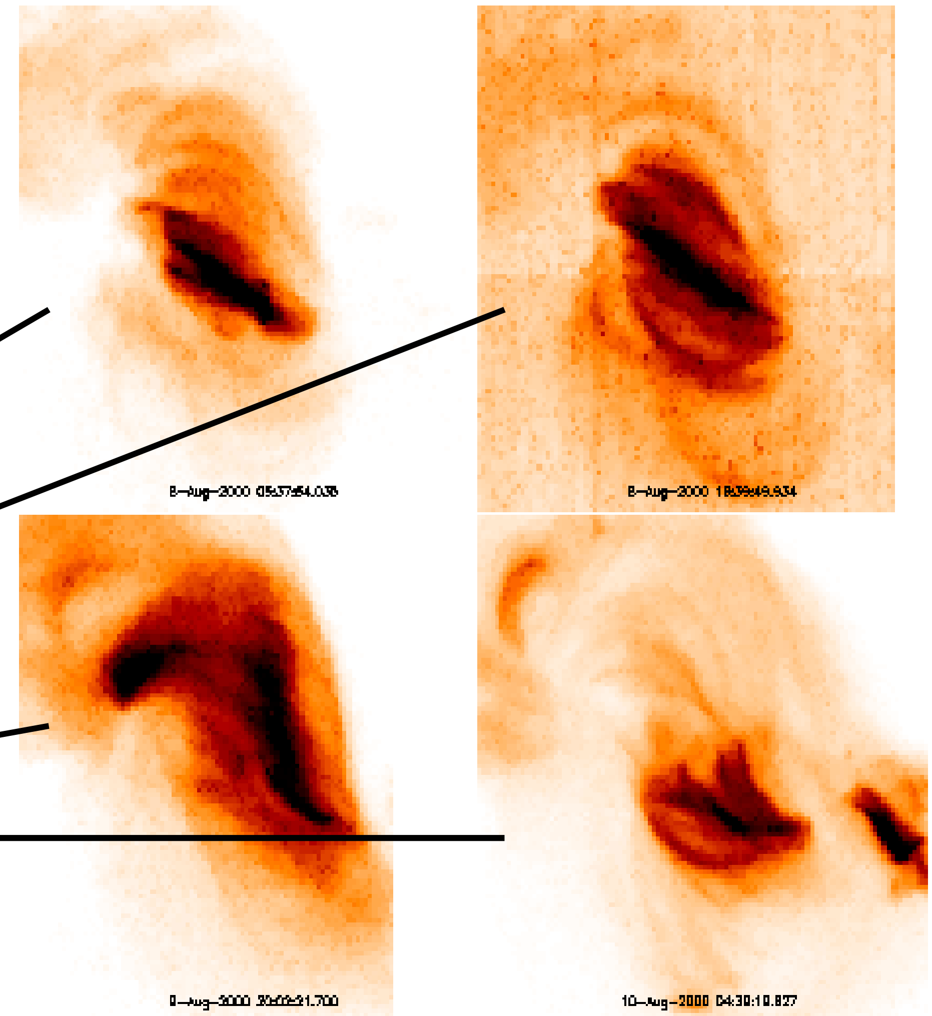

Figure 2: A selection of corresponding Yohkoh/SXT observations showing that the active region is initially unstressed, but as the rotation occurs a sigmoid forms and then dims, probably due to cooling, after the bulk of the rotation takes place.

Energization

- We can estimate the changes in the electromagnetic energy flux in the twisted loops by using the integral of the Poynting Flux Density **S** through some area of the photosphere represented by a vector **ds** normal to the surface:

$$\oint \vec{S} \bullet \vec{ds} = \frac{c}{4\pi} \oint \left(\vec{E} \times \vec{B}\right) \bullet \vec{ds} = -\frac{1}{4\pi} \oint \left[\left(\vec{v} \times \vec{B}\right) \times \vec{B}\right] \bullet \vec{ds} \approx -\frac{1}{4\pi} v_\phi B_z B_\phi \pi \left(r_b^2 - r_a^2\right)$$

- where **v** is the rotational velocity, which is in the azimuthal direction and counter clockwise; **B** is the magnetic field vector (B_z, B_r, B_ϕ); and **E** is the electric field vector; r_b, r_a are the radii of the outer and inner sides of the annulus defining the approximate region of the foot points of the twisting loops.
- The average rotational speed v comes from our August 8-10, 2000 rotational speed analysis in the penumbra, assumed now to move as a rigid body with the magnetic fields frozen in. We use the penumbral speeds because the foot points appear to be in the penumbral region of maximum speed, as shown in the next figure by the light blue circles of radii r_b = 12'', r_a = 8''.
- We obtained the magnetic field values from Mees vector magnetograph data using a magnetogram at 19:12 on August 8. We averaged the product of B_z B_ϕ within the penumbral annulus between r_a and r_b.

Energization

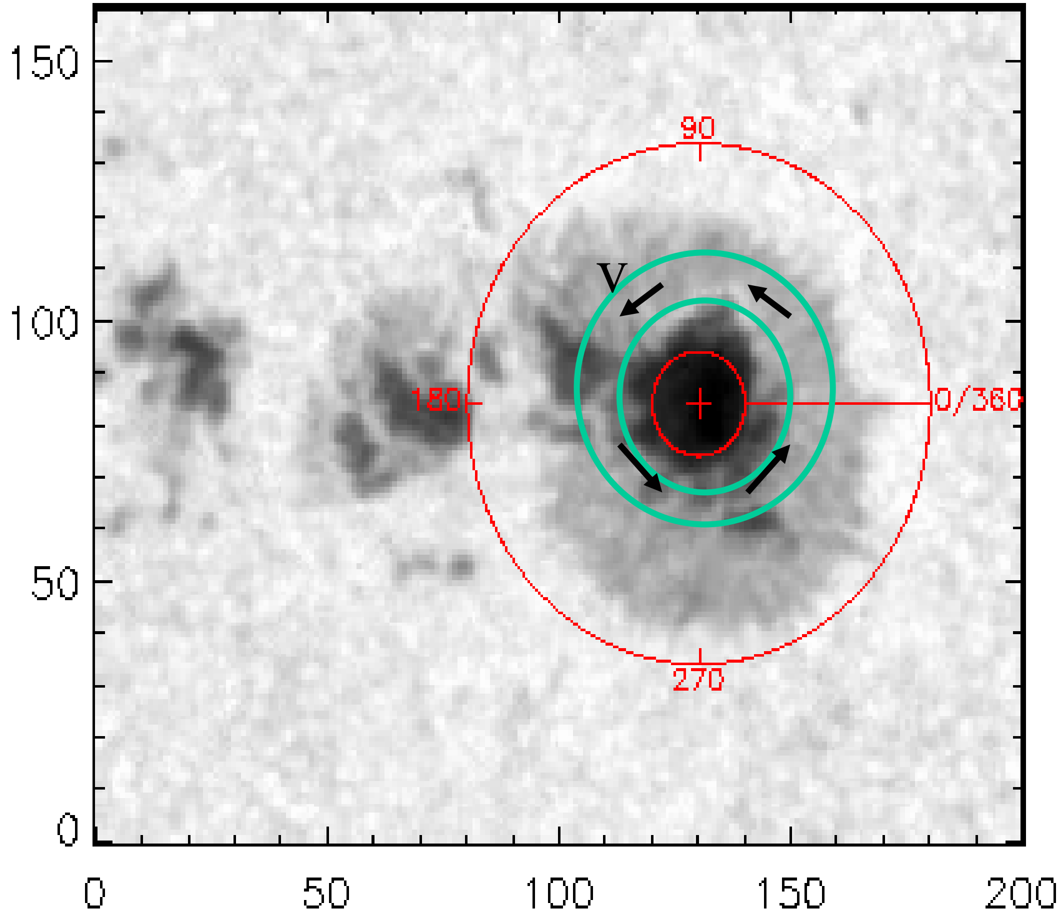

Helicity Injection

Rate of Helicity Injection: from Kusano et al., 2002

$$\dot{H}_t = -2\int (v_\phi \cdot A_p) B_n dS \approx -2B^2 L < v_\phi > = -8\times 10^{35} < v_\phi (\deg/hr) >$$

Total Injected Helicity:

$$H_t = \int \dot{H}_t dt = -8\times 10^{35} \int < v_\phi > dt$$

Helicity charging and instability:

Rust and Kumar (1994a) find a simple relationship between the helicity, H_t and the flux, ϕ, $H_t(t) = \frac{L(t)\alpha\varphi^2}{2\pi}$ for a helical fluxrope model.

$\phi \sim 6 \times 10^{19}$ Mx

where L is the loop length and α is the force-free parameter. Rust and Kumar (1994b) calculated that a constant α fluxrope becomes unstable for $L\alpha > 3.7\pi$ or $H_t > 1.85\phi^2$. This compares favorably with the criterion for MHD instability at $H_t > 1.25\phi^2$ of Hood (1991).

In the figures we show both limits and their relationship to the injected helicity.

Aug 8-10 2000: Energization and Helicity Charging

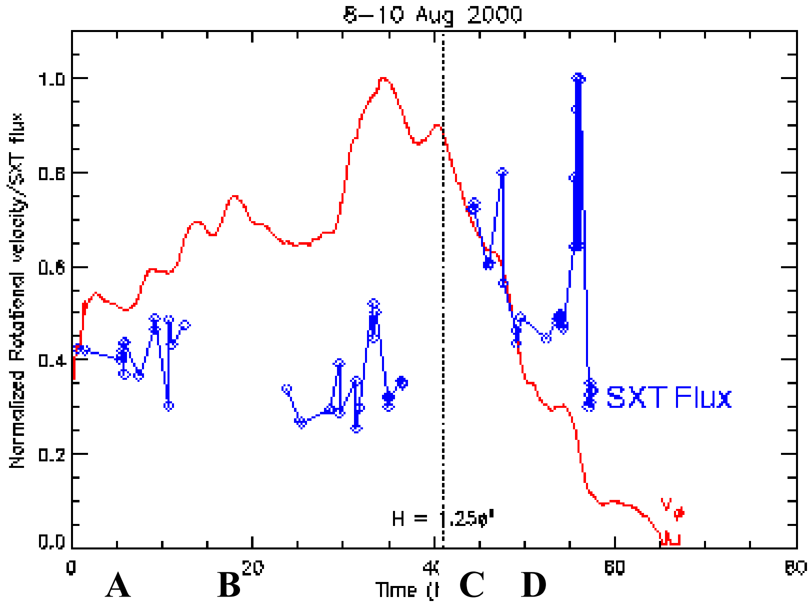

SXT Flux determined from composite (long+short exps.) images

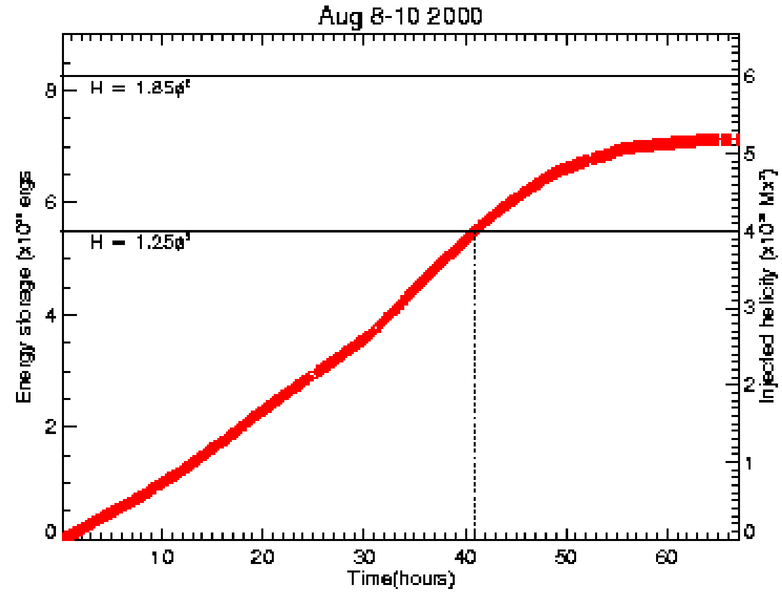

Cumulative energy storage and helicity for X-ray sigmoid

As helicity injection exceeds the critical limit of Hood (1991), $H_{crit}=1.25\phi^2$, sigmoid reaches maximum spatial extent (Frame C). However, the upper limit corresponding to the Rust and Kumar (1994a) instability criterion is not attained.

ϕ = magnetic flux

August 15-18, 1999
(WL, 1600 A, 171 A)

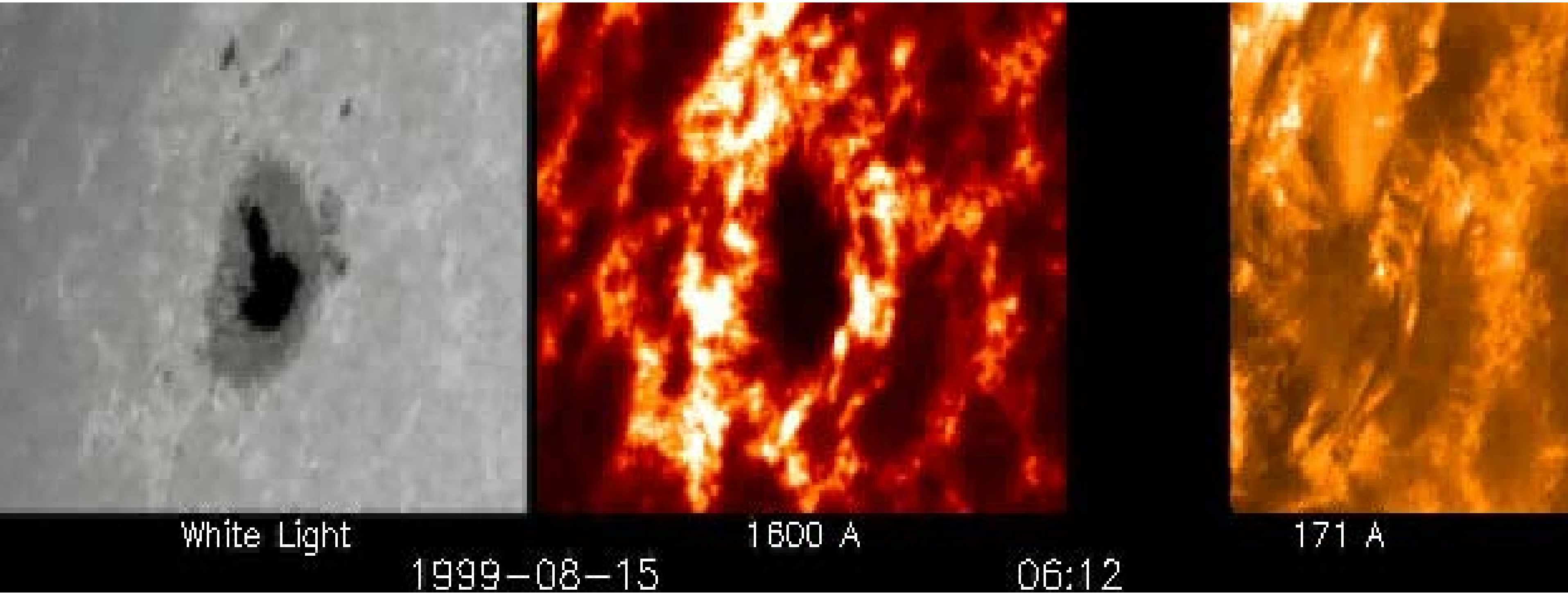

August 15-18, 1999

(WL 1600 A, 171 A)

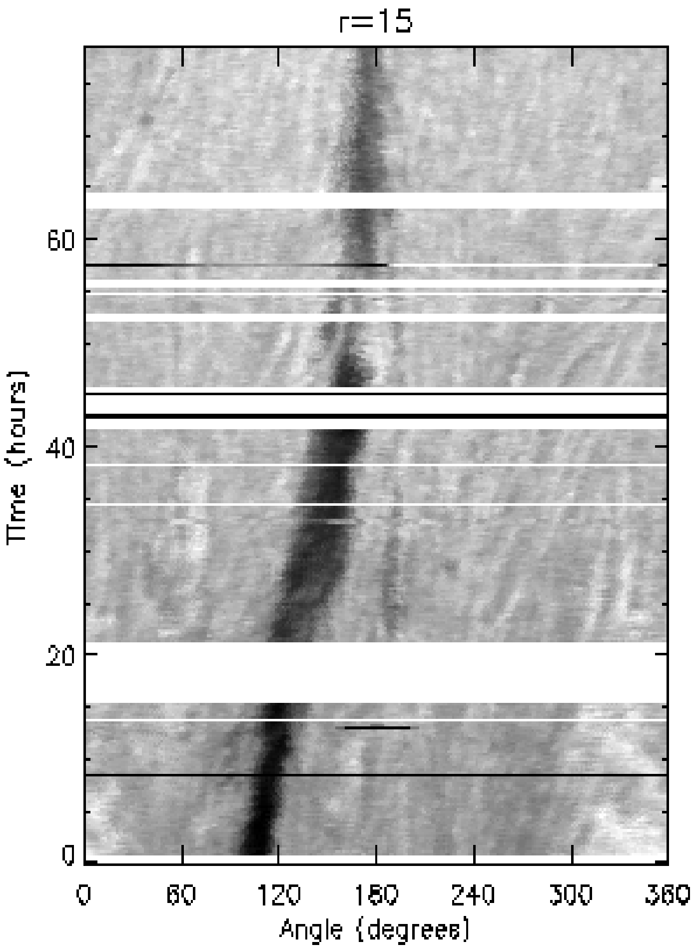

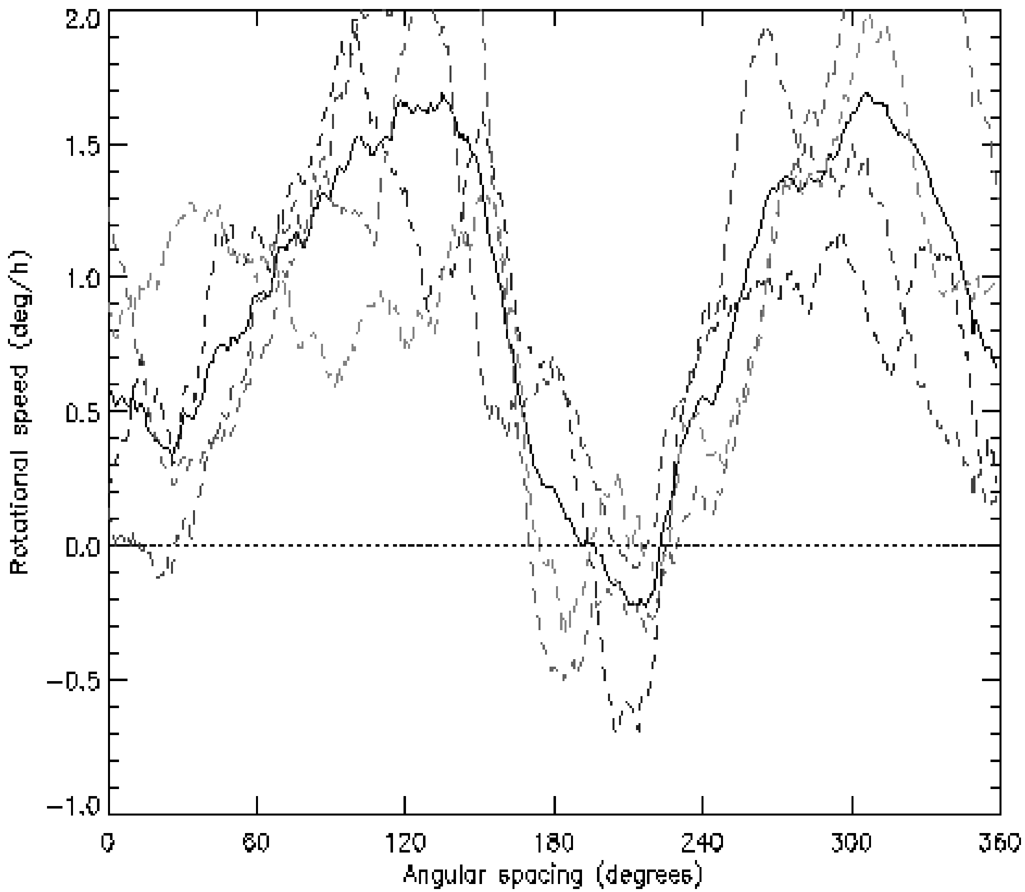

August 15-18, 1999

A sigmoid structure can be seen in the Yohkoh/SXT images (top and third row), which are compared to H-alpha images (second and last rows) from Big Bear Solar Observatory. The images are for the six August days of 16-21 at ~14:00-16:00 UT. (Figure taken from Yohkoh/SXT Science Nugget of December 17, 1999.)

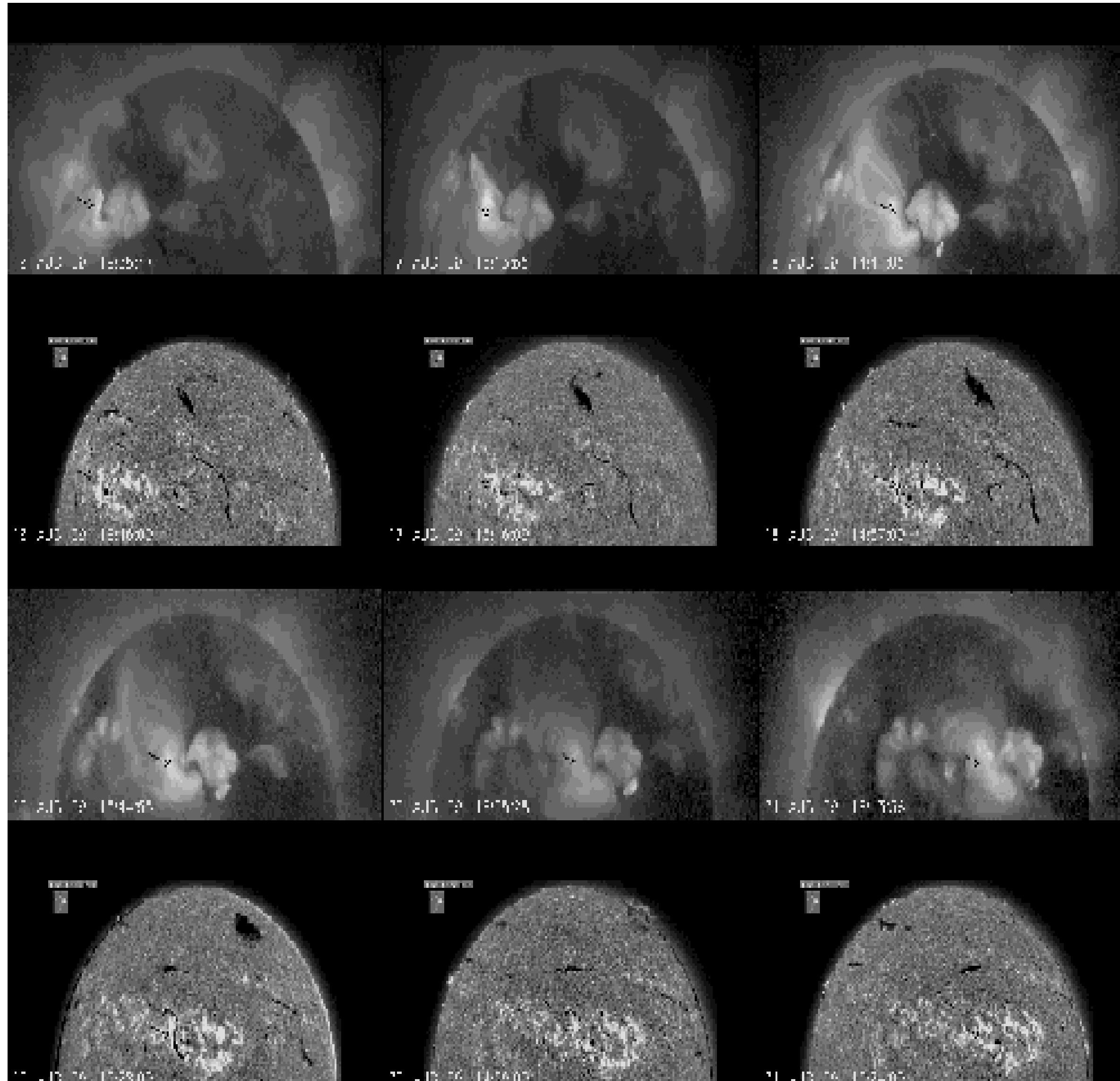

Aug 15-18 1999: Energization and Helicity Charging

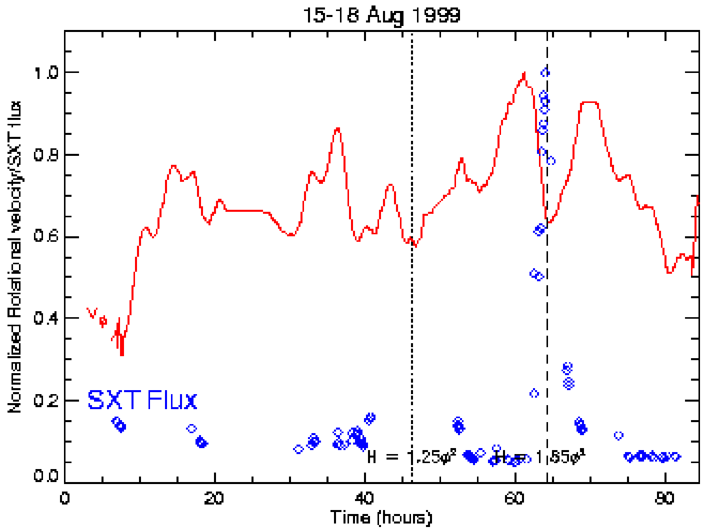

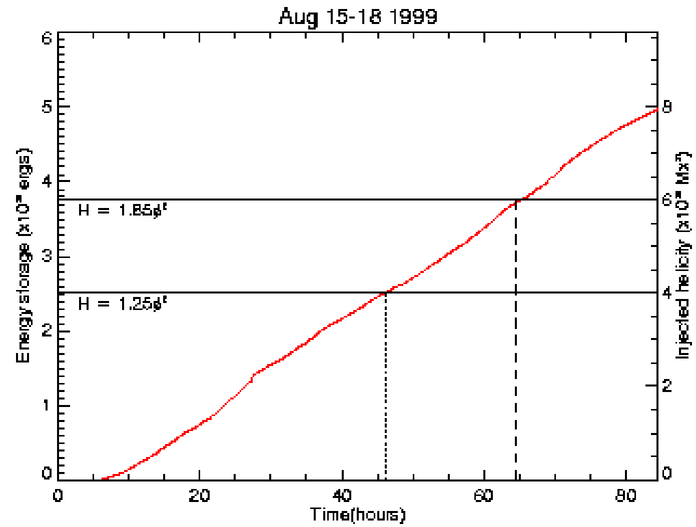

Cumuulative energy storage and helicity for X-ray sigmoid

In this case, helicity injection exceeds the Rust and Kumar (1994b) instability criterion, $H_t > 1.85\phi^2$. At this time the X-ray sigmoid exhibits a substantial growth in brightness and erupts (see Gibson et al., 2002).

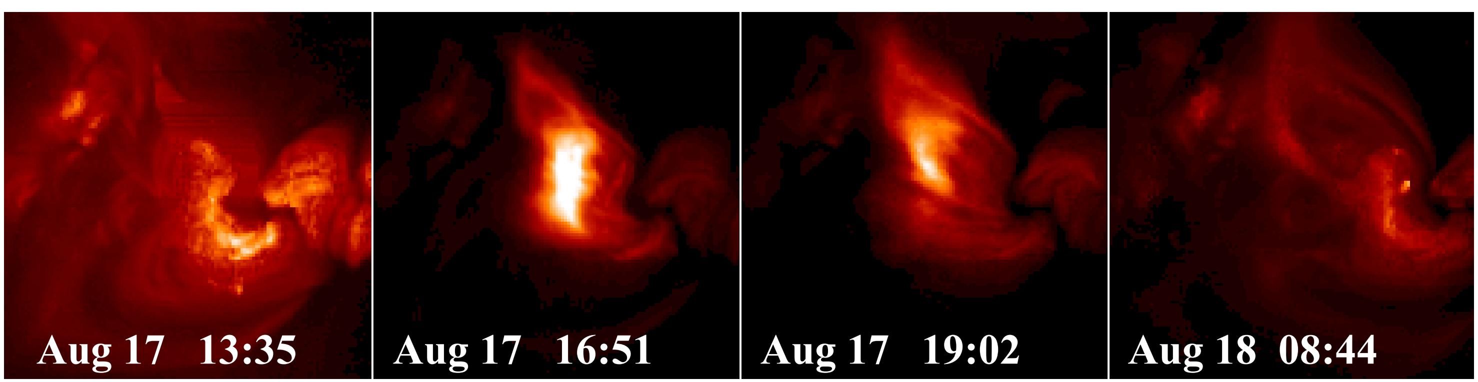

HOUR	**61.5**	**65**	**67**	**81**

Conclusions

- **Results are preliminary but seem to indicate that helicity charging generated by sunspot rotation is critical to the eruption (or `not') of their associated X-ray sigmoids.**

- **For both sigmoids considered the helicity injection due to the observed sunspot rotation exceeded the critical limit for instability defined by Hood (1991), $H_{crit} = 1.25\phi^2$. But only in the sigmoid spanning Aug 17 1999 did the helicity injection exceed the instability limit identified by Rust and Kumar (1994b) (RK), $H_{crit} = 1.85\phi^2$. The attainment of the Hood critical helicity was accompanied by a brightening of the sigmoid in the Aug 2000 case, while the attainment of the RK critical helicity in the Aug 1999 case resulted in an eruption of the sigmoid.**

- **The evolution of a sigmoid prior to eruption typically shows significant but low level activity (C-flares, X-ray brightness variations). This needs further investigation but may be a result of quasi-steady dissipation of the type described by Somov and Syrovatskii (1979), which `bleeds' energy from the sigmoid, heating it to X-ray temperatures, without significantly impacting its overall growth in growth in free energy and helicity.**